Desalination and Water Treatment
www.deswater.com
doi: 10.5004/dwt.2022.28386

258 (2022) 43–54
May

Application of heat-mass transfer analogy for understanding the mechanism of fouling control in a submerged flat sheet microfiltration membrane

Tahir Maqsood Qaisrani[a,*], Aiman Fatima[a], W.M. Samhaber[b]

[a]*Pakistan Institute of Engineering and Applied Sciences, P. O Nilore, Islamabad, Pakistan, Tel. +92-51-9248714; Fax: +92-51-9248600; emails: tmqaisrani@pieas.edu.pk (T.M. Qaisrani), uetian.aiman@gmail.com (A. Fatima)*
[b]*Institute of Process Engineering, A-4060 Leonding, Welser Str. 42, Johannes Kepler University, Linz, Austria, email: wolfgang.samhaber@jku.at*

Received 4 October 2021; Accepted 24 February 2022

ABSTRACT

Experiments of microfiltration enhanced with air dispersion were carried out through a submerged flat sheet membrane using commercial yeast suspension. In the experiments, the effect of hydrodynamic parameters like liquid flow velocity, air flow rate and aerator size were examined on flux control of fouling for different feed concentrations at constant transmembrane pressure. The classical heat and mass transfer analogy was applied to get an insight into the mechanism of fouling control in single and two-phase flow systems. The experimental results show that: (a) air dispersion reduced the particle fouling on membrane surface thus causing permeate flux enhancement for any value of air flow rate and for any feed concentration. A maximum flux enhancement factor of 270% was achieved for feed concentration of 25 g/L whereas as it was 60% for feed concentration of 1 g/L at an optimum air flow rate of 64 L/min. (b) Convective back transport of solids from membrane surface due to shear forces generated during two-phase flow was found to the be most significant phenomena of fouling control in submerged flat sheet microfiltration membranes. (c) The classical heat and mass transfer analogy successfully provided the explanation of phenomena of convective back transport of solids due to gas-liquid two-phase flow.

Keywords: Submerged flat sheet membrane; Microfiltration; Heat and mass transfer analogy; Fouling control; Two phase flow; Convective back transport

1. Introduction

Microfiltration (MF) is a membrane separation process for physical separation of solids from the liquid. Its wide range of operation for very fine solids to very coarse particles has made MF more a subject of interest for almost all process industries involving solid–liquid separation. MF can be used in process industries like wastewater treatment, water purification, semiconductor, fruit juice, brewery, pharmaceutical industries. Its most recent application is pretreatment of sea water for reverse osmosis operations. The major problem associated with MF separation process is membrane fouling which can be external, internal or both. Fouling is undesired in membrane processes as it not only hampers the membrane performance due to deposition of solids on the membrane surface but also decreases the membrane life due to chemical cleaning. Control of fouling is therefore always a matter of prime interest for reasons of process efficiency. In last four decades, different fouling control techniques have been suggested by various researchers. These techniques include: use of turbulence promoters [1]; dynamic filtration [2]; pulsating flows [3]; helical baffles [4], jet flows [5]; vortex waves [6]; baffles as well as electric and ultrasonic [7] and surface and feed treatments [8]. Although process efficiency can be improved by all aforesaid techniques,

* Corresponding author.

but the industrial application of such techniques is limited by technological aspects. Another technique which has attracted the attention of researchers in recent years is continuous injection of gas/air in the feed stream. This technique was first used by Imasaka et al. [9]. In this technique, gas/air is dispersed in the liquid stream to generate two-phase flow which produces very high turbulences along the membrane surface. This high turbulence on the membrane surface reduces the deposition of solid particles on membrane surface and resultantly, the permeate flux increases. The advantages of significant flux enhancement and reduced energy cost associated with this technique have encouraged further activity. The majority of the studies on gas dispersion have been conducted for the membrane applications in which the feed suspension flows inside the membrane module, that is, tubular and hollow fiber membrane modules. To date, more attention has been given to the application of gas–liquid two-phase flow in submerged hollow fiber systems. Limited data of a fundamental nature have been published for bubble interaction with submerged flat sheet membranes. This limited data has come from the commercial suppliers of membrane systems and, as a result, much of the know-how is not published [10]. It is interesting to note that there is no published work regarding effectiveness of gas-liquid two-phase in spiral wound modules except only one study by Qaisrani and Samhaber [11]. The probable reason is that spiral wound elements are considered to be good in generating high flow instabilities without application of two-phase flow. However, Qaisrani and Samhaber [11] have shown in their study that gas–liquid two-phase is also effective in enhancing the membrane performance for open-channel spiral wound membrane module.

Lee et al. [12] first conducted experiments with gas bubbling in a flat sheet module to enhance the ultrafiltration of bacteria suspension. They used flat sheet membranes with different pore sizes and they were able to improve the permeate flux by up to 100% using a 300 kDa PS ultrafiltration membrane and 30% by using a 0.2 μm microfiltration membrane. Mercier-Bonin et al. [13] used flat sheet ceramic membranes for microfiltration of yeast suspension with air bubbling. They used a test cell of 85 mm × 85 mm × 0.6 mm. A flux increase of 4 times was reported for the applied process conditions with two-phase flow. Recently Ndinisa [10] used air bubbling in submerged flat sheet MF membranes for investigating the influence of hydrodynamic parameters and finding out the flux enhancement mechanism in these membranes. He used commercial yeast as model suspension. He showed that average wall shear stress increased with air flow rate and this increase in wall shear stress caused a reduction in fouling on the membrane surface and an enhancement in the permeate flux. He linked the wall shear stresses with bubble size with the help of computational fluid dynamics (CFD) simulations. Most recently, Sriprasert [14] studied the influence of two-phase flow on fouling of submerged flat sheet anaerobic bioreactors for dairy waste water treatment. He used non-adsorbent particles coupled with conventional gas sparged AnMBR (GSAnMBR) functioning as a three-phase (solid/gas/liquid) flow for fouling mitigation and flux enhancement purposes. He showed reduction in membrane resistance of 40%–88% due to scouring of particles. In the latest review on the behavior of suspensions and macromolecular solutions in cross-flow microfiltration by Chew et al. [15], the authors are of the view that the use of molecular dynamics simulations to model transport and fouling represents a major advance, providing insights not possible through experiments.

It is established that the internal fouling or pore blocking can only be removed by chemical treatment or back flushing. However, the hydrodynamic parameters like cross flow velocity, air flow rate, nozzle size and feed concentration are considered to have a great influence on the external fouling properties. There is a number of mechanisms reported in the literature for the enhancement of the permeate flux and mitigation of external fouling with air dispersion in flat sheet membrane modules. A number of mathematical models and empirical relations have been proposed for understanding the phenomena of external fouling in flat sheet microfiltration membranes. However, there is no clear agreement among the researcher on exactness of any mechanism. Most of the authors consider wall shear stress to be the primary factor for minimizing the fouling on the membrane surface while others think that it is flow reversal which is causing this effect. Furthermore, there has been no published work on application of heat and mass transfer analogy for explaining the mechanism of back transport of solids from the membrane surface towards the bulk. Therefore, the aim of this study is to investigate the effects of different hydrodynamic parameters on membrane fouling and to apply heat and mass transfer analogy in order to get into an insight of the fouling control mechanism in a submerged MF flat sheet membrane.

1.1. Heat and mass transfer analogy

If two or more processes are governed by dimensionless equations of the same form, the processes are said to be analogous. It is an established fact that heat and mass transfer processes are analogous for same geometric conditions. Heat transfer is governed by dimensionless Nusselt number (Nu) whereas the mass transfer is governed by dimensionless Sherwood number (Sh). The general forms of these numbers are given in Eqs. (1) and (2) respectively.

$$\mathrm{Nu} = \frac{hL}{k_f} \tag{1}$$

$$\mathrm{Sh} = \frac{h_m L}{D} \tag{2}$$

where h is convective heat transfer coefficient, h_m is mass transfer coefficient, L is characteristic length, k_f is thermal conductivity of the fluid and D is diffusion coefficient. Nusselt number is function of Reynolds number and Prandtl number whereas Sherwood number is dependent upon Reynolds number and Schmidt number according to Eqs. (3) and (4):

$$\mathrm{Nu} = C\,\mathrm{Re}^m\,\mathrm{Pr}^n \tag{3}$$

$$\mathrm{Sh} = C\,\mathrm{Re}^m\,\mathrm{Sc}^n \tag{4}$$

where *C*, *m* and *n* are constants which are dependent upon the operating conditions irrespective of fluid properties.

The heat and mass transfer analogy has been successfully applied to many other processes. Steeman et al. [16] studied the applicability of the heat and mass transfer analogy in indoor air flows. They applied CFD simulations to confirm the results of heat and mass transfer analogy. In this study they found that heat and mass transfer analogy can give accurate results provided the boundary conditions do not change. Miller and Atchley [17] applied this analogy to a low slope roof for estimation of heat transfer through the roof. They developed a mathematical correlation in order to take into account the condensation and evaporation effects of the moisture present on the roof surface. They found that heat and mass transfer analogy along with their developed correlation gave only 5% error as compared to the experiment data. Farinu [18] applied this analogy in deep frying of sweet potatoes. He applied computer simulations for calculating mass transfer coefficient whereas he calculated heat transfer coefficient experimentally from frying of potatoes. He found the same trend of increasing and heat and mass transfer with increase in temperature and decreasing trend for both with increasing the size of the potato chips.

Heat and mass transfer analogy is used in different systems to convert heat transfer coefficients into mass transfer coefficients in order to evaluate the transfer of mass from a surface. This analogy is used mostly in those systems where mass transfer cannot be measured or calculated. Mass transfer from the membrane surface to the bulk of the suspension in a flat sheet membrane module is similar to the classical problem of forced convection flow over a flat plate. In both heat and mass transfer, the hydrodynamic factors like cross flow velocity, air flow rate, bubbling frequency and size of the nozzle play a significant role in controlling the heat and mass transfer from the surface. The use of heat and mass transfer analogy in membrane processes for quantification of convective back transport has not been reported so far. This work can be considered to be first of its kind in this regard. It is not possible to measure the back transport of the solids from the membrane surface to the bulk of the suspension in any microfiltration membrane module. The heat and mass transfer analogy can help to estimate accurately the phenomena of back transport of the solids and thus can explain the mechanism of the flux enhancement due to gas-liquid two-phase flow.

2. Experimental

2.1. Materials

Fig. 1a shows the schematic diagram of the experimental set-up used for filtration experiments whereas the experimental setup for heat transfer experiment is shown in Fig. 1b. The permeate was collected from the membrane by applying a suction pressure whereas the process tank was kept open to the atmosphere. The system was operated at a constant pressure whereas permeate flux decreased with time.

A PES microfiltration flat sheet membrane by Microdyn-Nadir, Germany was used with a nominal pore size of 0.2 μm. The new membrane is stabilized with glycerin which is washed away when membrane comes into contact with water. The membrane was fixed on a PVC flat sheet with epoxy glue in such a way that its top end opened in a pipe from where the permeate was to be collected. The membrane was suspended 100 mm above the bottom of the cell. The process feed cell was a rectangular in shape with total liquid capacity of 2 L. The feed suspension was filled up to 70 mm above the top of membrane unit. The total surface area of the membrane was 0.016 m^2. The channel gap,

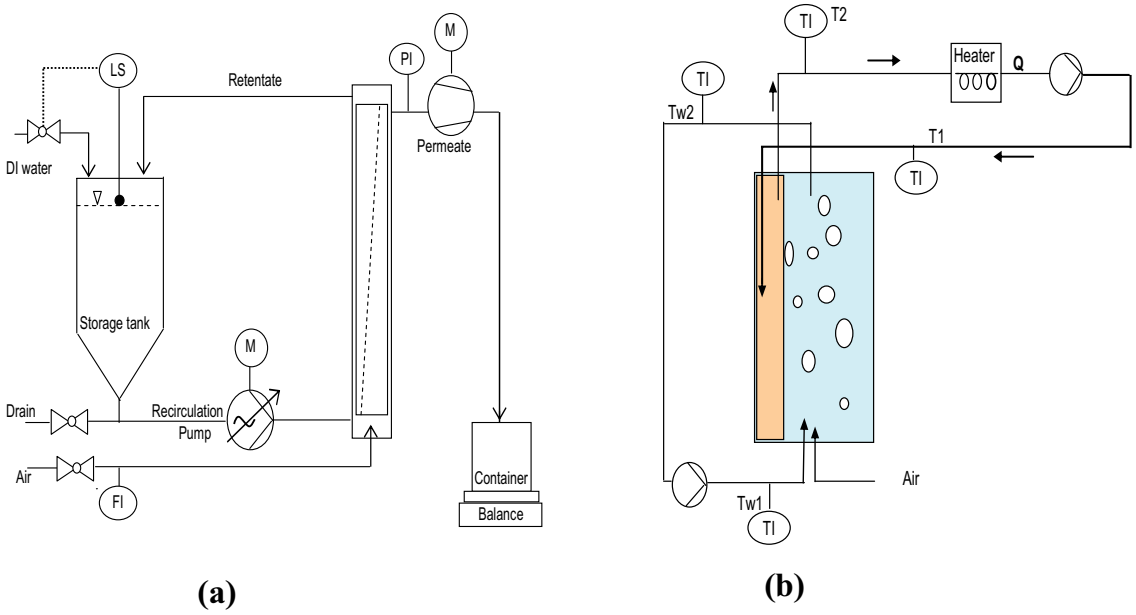

Fig. 1. Schematic diagram of experimental set-up: (a) filtration experiments and (b) heat transfer experiments.

that is, the gap between the membrane and the cell wall was 20 mm. Air inlet nozzles were fabricated by drilling holes in a 16 mm diameter PVC pipe.

Cylindrical nozzles were made by drilling 5 holes of same size on each tube. The holes were 10 mm apart. The PVC tube with nozzles was placed into the tank at a point which was 100 mm below the bottom of the membrane. The cylindrical nozzles were 0.5, 1.0, 1.5 and 2 mm diameter. The schematic diagram of the nozzle arrangement is shown in Fig. 2. The suspension for experimentation was made from commercially available bakers' yeast. Yeast of single commercial brand was used for all experiments of this study. Yeast was chosen as model suspension due to the reasons that it is easily available and also because it has properties which simulate those of mixed liquor, cell debris and extracellular materials (Ndinisa [10]). Atomic force microscopy (AFM) was used to determine the particle size and particle size distribution of the yeast cells. The average particle size of yeast was found to be 4.5 μm. A turbidity meter WTW-Turb 550 was used to measure the turbidity of the feed suspension and for determining the permeate quality. The concentration of solids was calibrated as function of turbidity for purpose of analysis of the data.

2.2. Experimental procedure

The permeate flux for pure water was measured by using Milli-Q pure water for the new membrane as a standard pure water flux. The yeast suspension was prepared by mixing the yeast into water with the help of a mechanical stirrer for half an hour. The yeast was not washed before preparation of the suspension. The feed concentration ranged from 1 to 25 g/L depending upon the experiment. The membrane module was inserted into the cell after transferring the suspension and air dispersion was started immediately after the transfer of the suspension. A vacuum pump by Vacuubrand, Germany with a suction capacity of 2.4 m^3/h was used for collecting the permeate into a glass vessel placed on the balance. A variable flow positive displacement pump was used for liquid feed circulation. The duration of all experiments ranges from 90 to 120 min. All the experiments were carried out under room temperature. Air was dispersed into both stagnant feed suspension and into circulating feed suspension in order to compare the effect of air dispersion in both systems. In order to keep the concentration of solids in the system constant, the same amount of water as that of permeate collected was added into the system by a level-controlled solenoid valve.

After each experiment, the membrane was washed with de-ionized water so that all the cake layer washed away with water and then was dipped into a 2% solution of enzymatic membrane cleaning detergent Ultraperm 53 by Henkel, Germany for 1 h. The temperature of this solution was raised to 50°C before the membrane was dipped into it. After 1 h, the membrane was rinsed with de-ionized water and then placed in 3% HCl solution for conditioning purpose for half an hour. The membrane was then rinsed with de-ionized water. This procedure restored the membrane permeability to almost 100% and membrane was found to be in similar conditions at the initiation of each experiment.

It is necessary to be mentioned here that experiments in this study were carried out at various concentrations of feed, that is from 1 to 25 g/L whereas for understanding the phenomena of fouling and its control, the data of feed concentration of 5 g/L was selected being the medium level of fouling. Therefore, results with feed concentration of 5 g/L are mostly presented and discussed in this study.

3. Results and discussion

3.1. Effect of cross-flow velocity on flux enhancement

It is important to investigate the effect of cross flow velocity on membrane performance as this is a commonly used technique to enhance the membrane performance in the industry. However, the feed concentration of 5 g/L was randomly selected for study of effect of cross flow velocity.

The flux enhancement factor ϕ is the factor which is considered as the measure of effectiveness of any flux

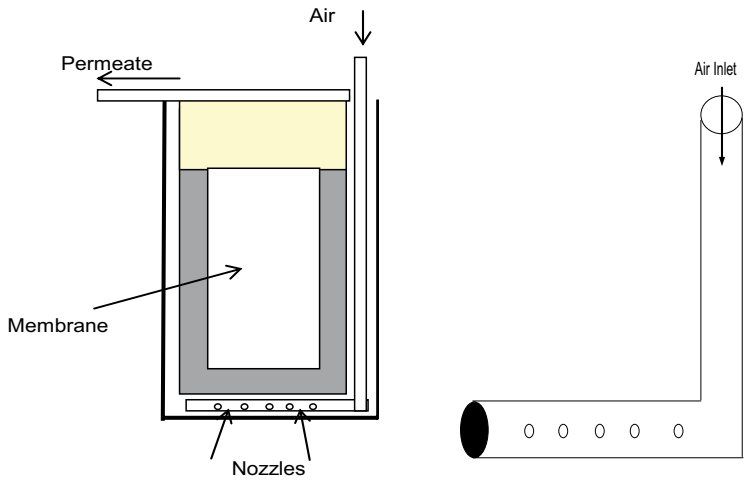

Fig. 2. Schematic diagram of the membrane cell and aerator.

enhancement technique. Flux enhancement factor for the method of increased cross flow velocity is defined as under:

$$\phi = \left[\left(\frac{\text{Flux at any cross-flow velocity}}{\text{Flux at lowest cross-flow velocity}}\right) - 1\right] \times 100 \quad (5)$$

Fig. 3 shows the variation of steady state flux and flux enhancement with cross flow velocity for a feed concentration of 5 g/L. A maximum flux enhancement of 65% and maximum steady state flux of 54 L/m² h-bar was achieved at feed-flow rate of 4.2 L/m beyond which both started to decrease.

3.1.1. Mechanism of flux enhancement with increased cross-flow velocity

It has been reported in many studies that increased cross flow velocity causes an increase in the wall shear force which hinders the deposition of solids on the membrane surface due to which permeate flux increases with increasing cross flow velocity. Hence increase in wall shear forces is attributed as the flux enhancement mechanism. Hwang et al. [19] showed with the help of a mathematical model, that wall shear forces are direct function of cross flow velocity and flux increased as cross flow velocity was increased. This implies that wall shear forces will keep increasing as cross flow velocity is increased and resultantly the permeate flux should also keep increasing. However, in contrary to these results, this study shows that there is a limiting value of cross flow velocity beyond which there is no further increase in the permeate flux.

For finding out the flux enhancement mechanism, two approaches have been used. The first approach is based on analysis of bulk feed concentration data. The data for bulk feed concentrations at the end of each experiment was collected and analyzed carefully for observing the effect of cross flow velocity on convective back transport of solids from the membrane towards the bulk feed suspension. Fig. 4 shows the effect of cross flow velocity on final bulk feed concentration at the end of each experiment. It can be seen from this figure that the number of particles kept increasing in the bulk feed with feed-flow rate due to convective back transport of the solids up to a feed-flow rate of 3 L/min and when feed-flow rate was further increased, the back transport of solids started to decrease sharply.

The second approach is based on study of heat and mass transfer analogy. The heat and mass transfer analogy was used to get an insight into this phenomenon of convective back transport of solids from the membrane towards the bulk of suspension. Heat transfer experiments

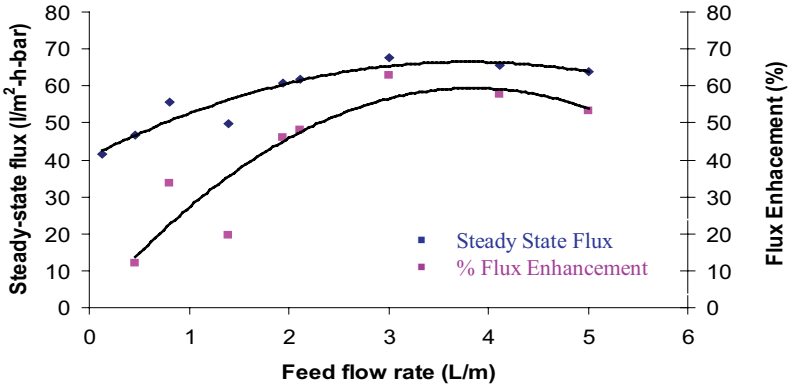

Fig. 3. Effect of cross flow velocity on steady state permeate flux and on flux enhancement factor at C = 5 g/L; ΔP = 0.4 bar.

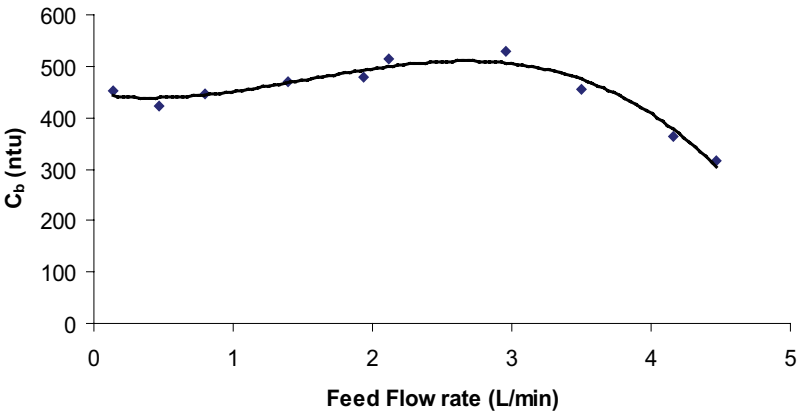

Fig. 4. Effect of feed-flow rate on bulk feed concentrations after 2 h operation at each feed-flow rate C = 5 g/L; ΔP = 0.4 bar.

were conducted in the similar operating conditions as that of filtration experiments. Fig. 5 shows the variation of heat transfer with liquid flow rate.

It can be seen from Fig. 5 that heat transfer coefficient increased with liquid flow velocity. The curve reveals that heat transfer will keep increasing till reaching the steady state value beyond which there will be no further increase in heat transfer. If we further increase the value of liquid flow rate beyond steady state, there would not be any increase in the value of heat transfer. The extrapolation of the curve also shows that there will be no further increase in the heat transfer if liquid flow rate is further increased which is logically true also as there will be no transfer of heat at steady state conditions. This is also evident from Eq. (6) where it can be seen that if temperature becomes constant (steady state) then heat transfer coefficient will remain constant even if liquid flow rate is increased. On the basis of this heat transfer relationship with liquid flow rate, mass transfer coefficient was calculated by using the following set of equations:

$$Q = hA\Delta T \tag{6}$$

$$\mathrm{Nu} = \frac{hL}{k} \tag{7}$$

$$\mathrm{Re} = \left(\mathrm{Nu} / 0.664\ \mathrm{Pr}^{1/3}\right)^2 \tag{8}$$

$$\mathrm{Sh} = 0.023\ \mathrm{Re}^{7/8}\ \mathrm{Sc}^{1/4} \tag{9}$$

$$\mathrm{Sh} = \frac{\beta d}{D} \tag{10}$$

Fig. 6 shows the relationship between liquid flow rate and mass transfer coefficient calculated based on heat-mass-transfer analogy. It becomes clear from this figure that the mechanism of fouling control and flux enhancement due to liquid flow velocity is convective back transport of the solids from the membrane surface towards the bulk suspension. When the liquid flow velocity is increased, it increases the convective back transport of the solids resultantly an increase in the permeate flux is obtained.

However, it is also important to note that after reaching a maximum at feed-flow rate of 3 L/min, the flux increase started to decline when feed-flow rate was further increased. This is due to the reason that increased turbulence due to increased feed flow velocity hindered the back transport of the solids and caused the compaction of the cake layer on the membrane surface. Thus the flux enhancement started to decline when feed-flow rate was increased beyond 3 L/min for this submerged flat sheet membrane module. This is analogous to the behaviour of convective heat transfer with liquid flow rate as transfer of heat also reaches its maximum at certain liquid flow rate beyond which there can be no further transfer of heat. The results of both approaches applied gives clear evidence that cross flow velocity increases the back transport up to a ceiling and this is the major mechanism of flux enhancement in single phase flow system.

3.2. Effect of air flow rate and nozzle size on cake layer and flux enhancement

The effects of air flow rate and nozzle size were studied by investigating a range of air flow rates on nozzles of different sizes. Experiments were carried out in the absence of liquid feed flow. For these investigations, air flow rates ranging from 4 L/min/m^2 of membrane area to 72 L/min/m^2 of membrane area while nozzle sizes of 0.5, 1.0, 1.5 and 2.0 mm were used. As the pore size of the membrane was less than the particle size, it was obvious that fouling of membrane with cake layer build-up would result and the effect of air flow rate and nozzle size would be more clearly identified. The rate of increase of the permeate flux was the main indicator of the effectiveness of air dispersion or nozzle size. If the fouling on the membrane surface is less, the permeate flux will increase and vice versa. Fig. 7 shows the typical results of steady-state permeate flux and flux enhancement vs. air flow rate for concentration of 5 g/L with nozzle sizes of 0.5, 1.0, 1.5 and 2 mm.

It can be seen in the figure that the steady state flux reached its peak at an air flow rate of 40–60 L/h and then started to decline when air flow rate was increased further. It can be seen from the figure that flux increased to a maximum at an air flow rate of 40 L/h beyond which it

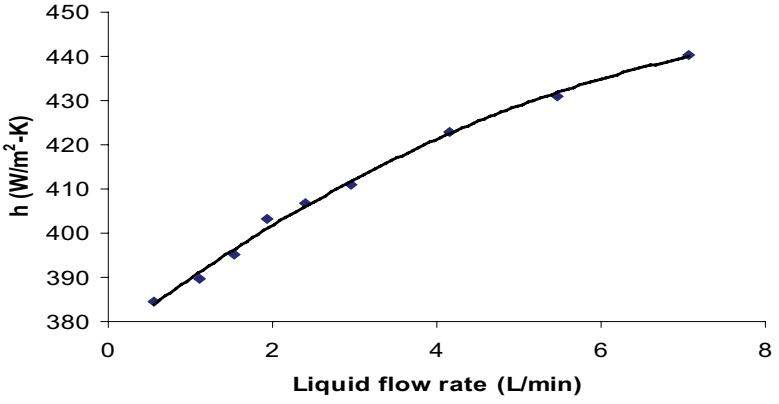

Fig. 5. Effect of liquid flow rate on heat transfer coefficient.

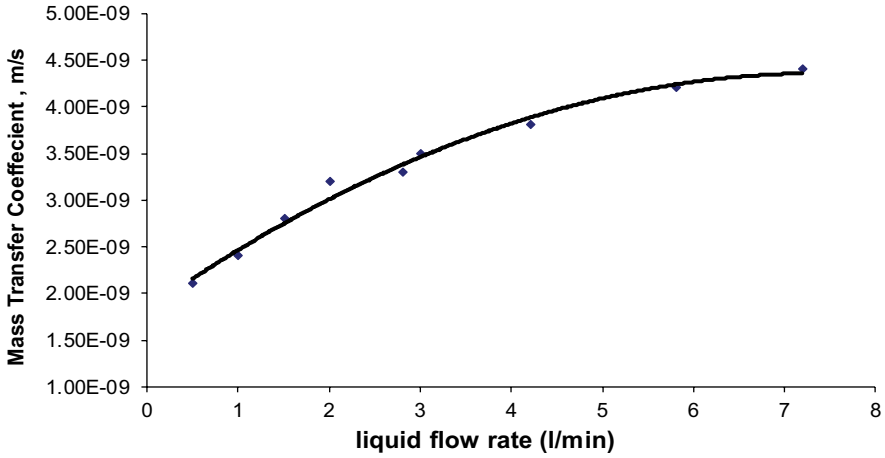

Fig. 6. Effect of liquid flow rate on mass transfer coefficient based on heat-mass transfer analogy.

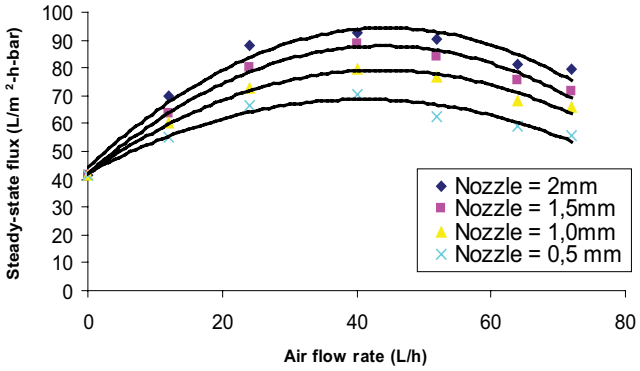

Fig. 7. Effect of air flow rate on steady-state permeate flux and on % flux enhancement; C = 5 g/L; ΔP = 0.4 bar.

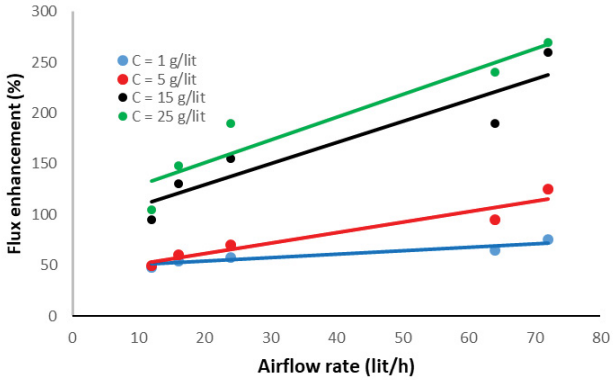

Fig. 8. Effect of air flow rate on flux enhancement (%) for 2 mm sized nozzle.

started to decline. This can be attributed to the reason that increased turbulence due to increased air flow velocity hindered the back transport of the solids and caused the compaction of the cake layer on the membrane surface. Thus the flux enhancement started to decline when air flow rate was increased beyond 40 L/h for this submerged flat sheet membrane module

Also it is evident from this figure that as the size of nozzle increases, the permeate flux also increases. Maximum flux enhancement was found to be with nozzle size of 2 mm. therefore, this nozzle size was used in other experiments too.

The flux enhancement factor ϕ is redefined here for an air-dispersed system as under:

$$\phi(\%) = \left[\left(\frac{\text{Flux with air dispersion}}{\text{Flux without air dispersion}}\right) - 1\right] \times 100 \qquad (11)$$

The extent of reduction of fouling was evaluated using flux enhancement factor for different feed concentrations and nozzle sizes. Fig. 8 shows how flux enhancement factor increased with air flow rate for nozzle of size 2 mm at different feed concentrations.

It can be observed from Fig. 8 that the flux enhancement is relatively lower for lower feed concentrations of 1 and 5 g/L but it is very profound for higher concentrations of 15 and 25 g/L. This shows that air dispersion is more effective for severe fouling conditions. Thus the increased air flow rate increased the effectiveness of bubbling for higher feed concentrations. These results are in contrast with the results of Ndinisa [10] as he observed less decrease in flux enhancement with air dispersion at higher feed concentrations as compared to lower feed concentrations. Ndinisa [10] used nozzle size of 0.5 mm and an air flow rate of 2 L/min with. Whereas in our study, a bigger nozzle of 2 mm diameter was applied with half the flow rate of Ndinisa [10]. Now it is a proven fact that larger the size of nozzle, bigger would be the size of bubbles. It is also established that bubble size and bubble size distribution are strongly dependent upon the air flow rate and the nozzle size. Resultantly, the bubble size plays a very significant role in determining the bubble rise velocity and the trajectory along which a bubble travels in the liquid. This implies that with increase in air flow rate and nozzle size, the size of the bubble will increase which in turn will increase the bubble rise velocity and sideways oscillations. These sideways oscillations of the bubbles are very high for larger diameter bubbles and cause a high degree of flow instabilities and turbulence in the liquid. Hence strong instabilities mean

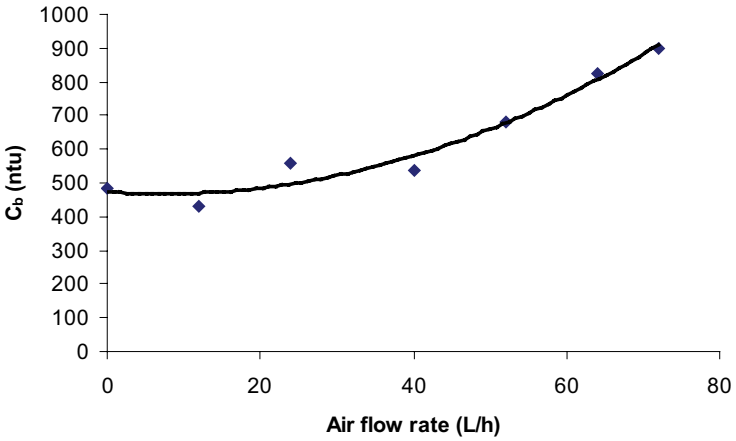

Fig. 9. Effect of air flow rate on bulk feed concentration after 2 h of operation for nozzle size = 2 mm; C = g/L; ΔP = 0.4 bar.

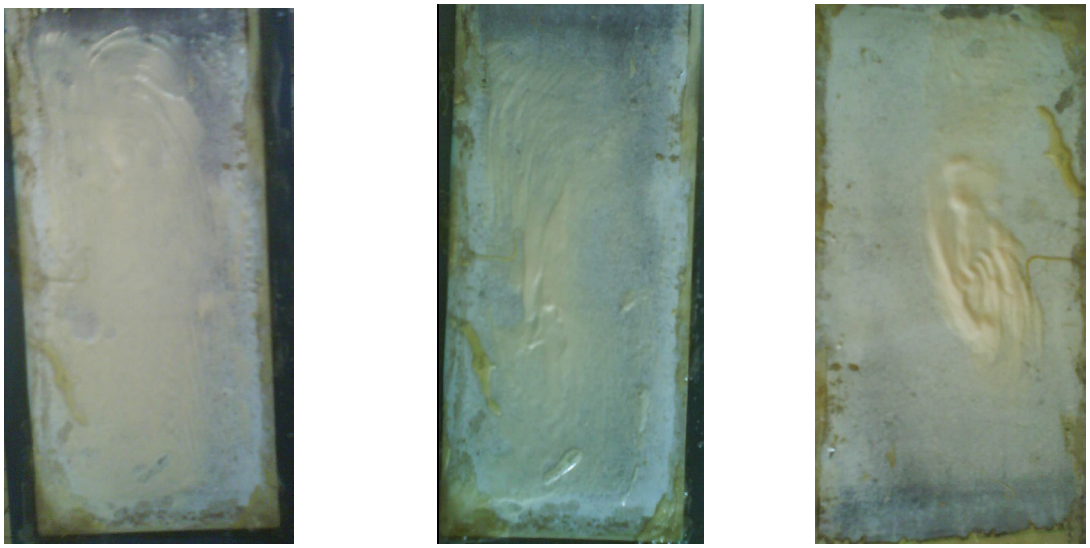

Fig. 10. Membrane surface at: a = 16 L/h; b = 40 L/h; c = 64 L/h for initial feed concentration = g/L.

lesser deposition of solids on the membrane surface and hence improvement in the permeate flux. As Ndinisa [10] applied a nozzle of 0.5 mm (4 times lesser than our set of experiments), therefore he obtained bubbles of very small diameter which in turn generated a lesser shear force. Hence he obtained results in contrast to this study.

In Fig. 8 the results presented are for maximum flux enhancement as it was seen in Fig. 7 that further increase in air flow rate will reduce the flux increase. Before reaching any conclusion for this effect, it is important to know the effect of air bubbling on bulk feed concentration. Fig. 9 shows the effect of air bubbling upon the final bulk feed concentration after 2 h of operation, that is, on steady-state conditions. From this figure, it is clear that as air flow rate increased, the concentration of solids in the bulk feed suspension also increased. This implies that there should be very less deposition of solids on the membrane surface. In order to verify this assumption, the membrane surface was analyzed physically at air flow rates of 16, 40 and 64 L/h. It can be seen in Fig. 10 that cake layer is apparently reduced to minimum for an air flow rate of 64 L/h (Fig. 10c) whereas membrane surface is fully covered with cake at lowest air flow rate of 16 L/h (Fig. 10a).

This implies that if there is no cake layer then there should not be any decrease in flux for higher air flow rates. However, this was not the case as seen in Fig. 7. The permeate flux started to decrease after reaching a maximum at air flow rate of about 40 L/h. this can be explained with the concept of bubble size increase with increase in air flow rate in two-phase flow. It is an established fact that when air flow rate increases, the bubble size also increases; which means that after the optimum air flow rate of 64 L/h, the size of the bubbles becomes so big that it starts to hinder the liquid to reach the membrane surface, that is, the bubbles act as cushion along the membrane surface so that permeation is decreased and the permeate flux decreases with increase in air flow rate beyond an optimum value of air flow rate.

3.2.1. Mechanism of fouling control and flux enhancement with air dispersion

The main objective of this study was to find out the mechanism for control of fouling with air dispersion in submerged flat sheet membrane system. Most of the studies on fouling control have been carried out in tubular and hollow fibre membrane modules. There is almost consensus of membrane researchers on the fouling control mechanism which says that air bubbling increases the wall shear stresses which helps to control the deposition of solids on the membrane surface. According to Cui et al. [20], the Taylor bubble in tubular membrane (which is of same diameter as that of the tube and is depicted in Fig. 11 is axis-symmetric, with a round nose and a relatively flat tail, and occupies most of the cross sectional area of the tube, while a thin liquid falling film flows around it adjacent to the tube wall. The liquid film accelerates as it moves downward, and then is injected into the liquid behind the bubble as a circular wall jet producing a highly agitated mixing zone in the bubble wake.

Another mechanism reported for tubular membranes is increased superficial velocity due to air bubbling in the membrane module. Bubbles of the size as that of tube diameter reduce the surface area of the membrane for the liquid thus increasing the superficial velocity of the liquid. In submerged flat sheet membrane modules, this mechanism also does not apply due to bubbles with sizes lower than the channel width.

As far as flat sheet membrane modules are concerned, there are only few countable studies. Mercier-Bonin et al. [13] with channel gap of 0.6 mm, Cabassud and Ducom [21] with channel gap of 5 mm and most recently Ndinisa [10] with channel gaps of 7 and 14 mm showed with the help of CFD simulations that wall shear stress was the main factor responsible for fouling reduction due to air bubbling in submerged flat sheet membranes. Ndinisa [10] was also of the view that apart from wall shear stress, liquid recirculation was another major factor responsible for the reduction of fouling on the membrane surface. For channel gap up to 10 mm, the bubbling flow pattern resembles with that of a tubular membrane as bubble diameter could become equal to that of channel gap and/or tube diameter. Therefore, the fouling control mechanism as reported by these authors is same as reported for tubular membranes.

The hydrodynamics change when the channel gap is such that bubble cannot attain the diameter equivalent to the channel gap. This fact has been reported by Ndinisa [10] as he used two channel gaps of 7 and 14 mm for his studies. He concluded with the remarks that it was impossible to differentiate between liquid recirculation and wall shear stress as fouling control mechanism for submerged flat sheet membrane module.

Another mechanism which has been given less importance is convective back transport of solids due to turbulences generated by air bubbling in the submerged flat sheet membrane modules. This study focuses on this fouling control mechanism. In order to validate this mechanism, heat and mass transfer analogy was used. Furthermore, the analysis of cake characteristics and membrane physical conditions were used to explain the convective back transport of solids from the membrane surface to the bulk suspension. The equations related to convective heat and mass transfer were utilized in order to find

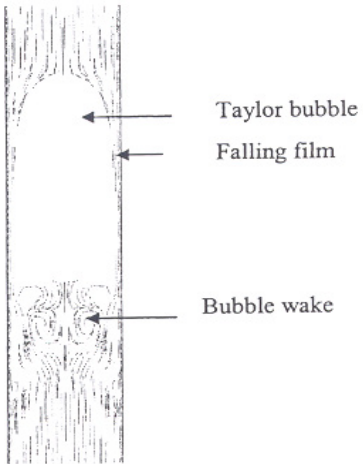

Fig. 11. Velocity field around a Taylor bubble with tube diameter of 10 mm in a stationary liquid. (*Source*: Cui et al. [20]).

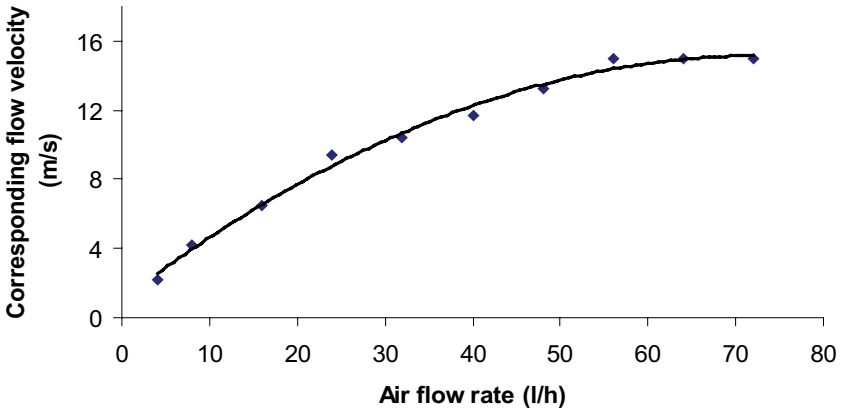

Fig. 12. Corresponding flow velocity vs. air flow rate in a submerged flat sheet module geometry.

out the 'corresponding' liquid velocity generated by air bubbling in the stagnant liquid. For calculating the value of Nusselt number and corresponding Reynolds number, Eqs. (6)–(8) were applied whereas the corresponding velocity was calculated from Eq. (11).

$$V_{cor} = \frac{\mathrm{Re}\,\mu}{\rho L} \tag{12}$$

Fig. 12 shows the corresponding flow velocities for different air flow rates. These velocities were in a very high turbulent range. Eqs. (9) and (10) were used for calculating Sherwood number and mass transfer coefficient respectively.

Corresponding flow velocities increased with air flow rate up to a certain value and reached a plateau value. On the basis of these values of heat transfer and corresponding flow velocities, the values of mass transfer coefficient were calculated. Fig. 13 shows the relationship of air flow rate and mass transfer coefficient.

It becomes clear from Figs. 12 and 13 that as air flow rate increases, the corresponding flow velocity increases which in turn increases the mass transfer coefficient. This implies that convective back transport of solids increases with increasing the air flow rate and hence there is deposition of lesser cake mass. Resultantly, the permeate flux increases with air flow rate. It is also evident from these figures that air flow rate has a limiting value beyond which both corresponding flow velocity and mass transfer coefficient cannot increase. This implies that there should be an optimal value of air flow rate beyond which the permeate flux would not increase. This optimal value from heat and mass transfer analogy experiment comes out to be 70 L/h where the experimental results in Fig. 13 show a limiting air flow rate of between around 64 L/min which is quite close to that of calculated from heat and mass transfer analogy. The difference in the limiting value of air flow rate for experimental result and theoretical values can be due to difference in fluid properties used in these methods. For heat transfer experiments, pure water was used whereas in filtration experiments, yeast suspension was used which obviously changes the fluid properties of water. This can be explained as following.

As the air flow rate increases, the size of the bubbles will increase to such an extent that these larger diameter bubbles will start to offer a resistance to the permeation process by covering the membrane surface. However, the heat and mass transfer analogy gives an excellent insight for convective back transport of the solids from the membrane surface to the bulk of the feed suspension. The trends shown in experimental results of Figs. 13 and 14 are in good agreement to those attained from convective heat transfer experiments.

The back transport of solids was further proved when the data regarding the bulk feed concentrations was analyzed for higher feed concentrations. The values of feed concentrations were measured at the end of each experiment. Fig. 14 shows the variation of bulk feed concentration of suspension at steady-state flux value at different air flow rates for a nozzle of 2 mm size.

Fig. 14 shows that for suspensions of any initial feed concentration, the back transport of solids increases with air flow rate and reaches a maximum value for the range of air flow rates applied in this study.

3.2.2. Effect of feed-flow rate on flux enhancement in two-phase flow conditions

Experiments were also carried out for investigating the effect of liquid flow rate in presence of air dispersion on fouling control. The values of air flow rates were varied for two different liquid flow rates of 1.1 L/min and 2 L/min with Re equivalent to 3,300 and 6,000, respectively. It implies that the flow is already in turbulent state for both the liquid flow rates. Fig. 15 shows the variation of flux with air flow rate for at different liquid flow rates. The percent flux enhancement was highest at lower air flow rates and further increase in air dispersion caused the flux to reduce. It can be deduced that as flow regimes were already in turbulent state, the air bubbling at higher air flow rates did not help to increase the flux significantly. Rather lower air flow rates improved the permeate flux. There was a limiting value of air flow rate for both conditions beyond which the permeate flux enhancement decreased very sharply. The air bubbling was found to be effective for laminar flow conditions.

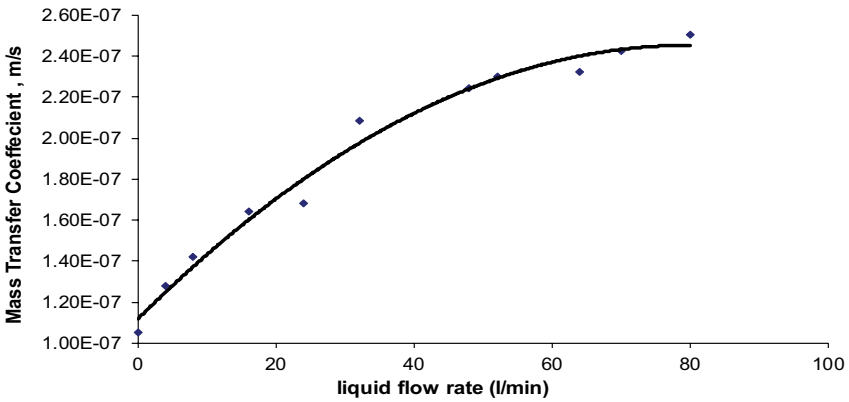

Fig. 13. Relation between air flow rate and mass transfer coefficient calculated from heat-mass transfer analogy equations.

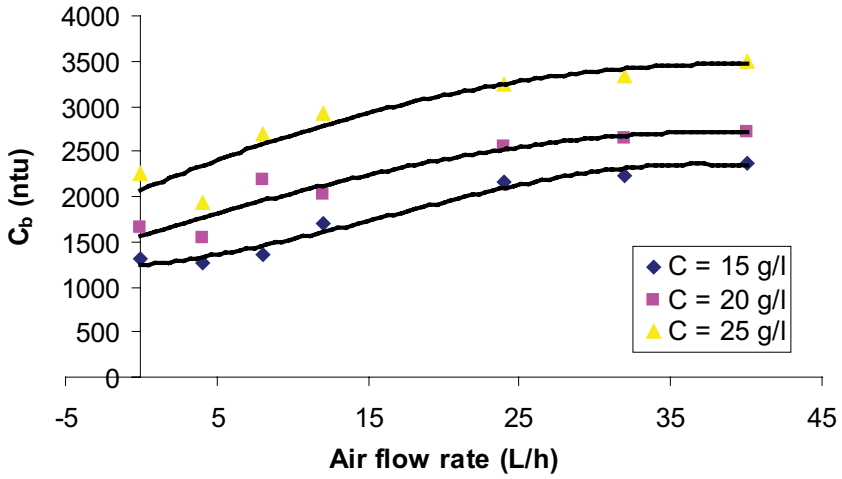

Fig. 14. Effect of air flow rate on bulk feed concentration at steady-state flux.

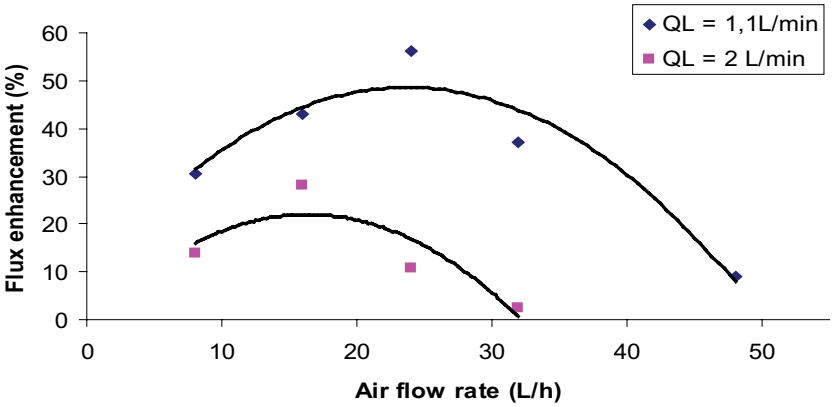

Fig. 15. Effect of liquid flow velocity on flux enhancement in presence of air bubbling; C = 5 g/L; ΔP = 0.4 bar; nozzle size = 2 mm.

The analysis of the bulk feed concentration at steady-state flux show that the bulk feed concentration continued to increase with air flow rate. Thus air bubbles in fact caused to cover the membrane surface and hindered the permeation process. Resultantly, the flux enhancement decreased with air flow rate after reaching the ceiling at lower air flow rates. This is similar to the case of filtration without liquid flow at higher air flow rates as shown in section 3.1.1 and Figs. 7 and 9. Similar results were obtained for higher bulk feed concentrations.

4. Conclusions

The main objective of this study was to find out the fouling control mechanism in single phase and two phase in a submerged flat sheet microfiltration membrane and explain the mechanism of fouling control with heat and mass transfer analogy. The key factors investigated are liquid flow rate, air flow rate, nozzle size and feed concentration. The performance of the process was evaluated in terms of change in steady-state flux, flux enhancement factor and reduction in cake layer on membrane surface. The important conclusions of the research presented in this study are summarized as following:

- Flux enhancement factor increased both with air and liquid flow rate and reaches a maximum for both the cases. A max flux enhancement factor of 250%, 220%, 150% and 70% was achieved for feed concentration of 25, 15, 5, and 1 g/L at an air flow rate of 64 L/m with 2 mm diameter air nozzle; whereas this factor was found to be 65% at a liquid flow rate of 4.2 L/m for feed concentration of 5 g/L.
- Flux enhancement factor is significantly higher, that is, almost 2 times higher for air-liquid two-phase system as compared to that of single phase flow at same feed concentration of 5 g/L.
- The convective back transport of solids was found to be the most significant phenomena induced by shear force air bubbles at membrane surface for control of fouling on surface of submerged flat sheet microfiltration membrane.
- The heat and mass transfer analogy successfully explained the phenomena of convective back transport of the solids from the membrane surface to the bulk which

in turn is one of the mechanisms of fouling control on membrane surface.
- The combination of single phase flow and two-phase flow was found to be least effective method for fouling control as only 50% of maximum flux enhancement factor was observed by this method.

5. Recommendations

From the outcome of the present work, some recommendations for the future work are proposed:

5.1. Characterization of gas-liquid two-phase flow

The results of this study showed that the permeate flux increased with air flow rate and nozzle size. In order to fully understand the mechanism of flux enhancement associated with air bubbling, it is necessary to characterize the two-phase flow for finding out the influence of two-phase flow on bubble characteristics like bubble size and shape, bubble size distribution, bubble rise velocity and bubble trajectory along the membrane surface. A CFD simulation study can help to understand the effect of bubble trajectory on hydrodynamics of the system and its possible effects on fouling control.

5.2. Optimization of membrane cleaning

The results of this study also show that air bubbling can physically displace the fouling layer. This implies that two-phase flow can be helpful in improving the membrane cleaning efficiency. The research work regarding membrane cleaning is underway and will be presented in some other paper.

References

[1] S.M. Finnigan, J.A. Howell, The effect of pulsatile flow on UF fluxes in a baffled tubular membrane system, Desalination, 79 (1990) 181–202.
[2] K.H. Kroner, V. Nissinen, H. Ziegler, Improved dynamic filtration of microbial suspension, Bio/Technology, 5 (1987) 921–926.
[3] B.B. Gupta, P. Blanpain, M.Y. Jaffrin, Permeate flux enhancement by pressure and flow pulsations in microfiltration with mineral membrane, J. Membr. Sci., 70 (1992) 257–266.
[4] B.B. Gupta, J.A. Howell, D. Wu, R.W. Field, A helical baffle for cross-flow microfiltration, J. Membr. Sci., 99 (1995) 31–42.
[5] G. Arroyo, C. Fonade, Use of intermittent jets to enhance flux in crossflow filtration, J. Membr. Sci., 80 (1993) 117–129.
[6] H.R. Millward, B.J. Bellhouse, I.J. Sobey, R.W.H. Lewis, Enhancement of plasma filtration using the concept of the vortex wave, J. Membr. Sci., 100 (1995) 121–129.
[7] J.-O. Kim, J.-T. Jung, I.-T. Yeom, G.-H. Aoh, Electric fields treatment for the reduction of membrane fouling, the inactivation of bacteria and the enhancement of particle coagulation, Desalination, 202 (2007) 31–37.
[8] I.G. Racz, J. Groot Wassink, R. Klaassen, Mass transfer, fluid flow and membrane properties in flat and corrugated plate hyperfiltration modules, Desalination, 60 (1986) 213–222.
[9] T. Imasaka, N. Kanekuni, H. So, S. Yoshini, Crossflow filtration of membrane fermentation broth by ceramic membranes, J. Ferment. Bioeng., 68 (1989) 200–206.
[10] N.V. Ndinisa, Experimental and CFD Simulation Investigations into Fouling Reduction by Gas-Liquid Two-Phase Flow for Submerged Flat Sheet Membranes, Ph.D. Thesis, University of New South Wales, Sydney, Australia, 2006.
[11] T.M. Qaisrani, W.M. Samhaber, Flux enhancement by air dispersion in cross-flow microfiltration of a colloidal system through spiral wound module, Global Nest J., 10 (2008) 461–469.
[12] C.K. Lee, W.G. Chang, Y.H. Ju, Air slugs entrapped cross-flow filtration of bacterial suspensions, Biotechnol. Bioeng., 41 (1993) 525–530.
[13] M. Mercier-Bonin, C. Lagane, C. Fonade, Influence of a gas/liquid two-phase flow on the ultrafiltration and microfiltration performances: case of a ceramic flat sheet membrane, J. Membr. Sci., 180 (2000) 93–102.
[14] P. Sriprasert, Application of Two and Three-Phase Flow in Submerged Flat-Sheet Anaerobic Membrane Bioreactors for Dairy Wastewater Treatment, Ph.D. Thesis, University of Southampton, UK, 2019.
[15] J.W. Chew, J. Kilduff, G. Belfort, The behavior of suspensions and macromolecular solutions in crossflow microfiltration: an update, J. Membr. Sci., 601 (2020) 117865, doi: 10.1016/j.memsci.2020.117865.
[16] H.-J. Steeman, A. Janssens, M. De Paepe, On the applicability of the heat and mass transfer analogy in indoor air flows, Int. J. Heat Mass Transfer, 52 (2009) 1431–1442.
[17] W.A. Miller, J.A. Atchley, A Correlation for Laminar, Low-Temperature, Gradient Heat and Mass Transfer Applied to a Low-Slope Roof, Oak Ridge National Laboratory (ORNL), Oak Ridge, Tennessee, USA, 2001. Available at: http://www.ornl.gov/~webworks/cppr/y2001/pres/111369.pdf
[18] A. Farinu, Heat and Mass Transfer Analogy Under Turbulent Conditions of Frying, M.Sc. Thesis, Department of Agricultural and Bioresource Engineering, University of Saskatchewan, Saskatoon, Saskatchewan, Canada, 2006.
[19] S.-J. Hwang, D.-J. Chang, C.-H. Chen, Steady-state permeate flux of cross-flow microfiltration, J. Membr. Sci., 98 (1995) 97–106.
[20] Z.F. Cui, S. Chang, A.G. Fane, The use of gas bubbling to enhance membrane processes, J. Membr. Sci., 221 (2003) 1–35.
[21] C. Cabassud, G. Ducom, Air Sparging in Flat Sheet Nanofiltration Membranes: Effect on Cake Deposit and on Concentration Polarization, 6th World Congress of Chemical Engineering, Melbourne, Australia, 2001, pp. 23–27.